Econ. Environ. Geol.
Vol. 32, No. 5 p. 445-454, 1999.

Mineralogy and Geochemistry of the Sanjeon Au-Ag Deposit, Wonju Area, Korea

Se-Hyun Kim*, Young-Cheon Choi* and Seung-Jun Youm**

ABSTRACT: The Sanjeon Au-Ag deposit consists of three subparallel hydrothermal quartz-calcite veins which filled fault-related fractures (generally N20° to 35°W-trending and 70° to 80° SW-dipping) within quartz porphyry. The vein mineralization shows an apparent variation of mineral assemblages with paragenetic time: (1) early, white quartz + pyrite + arsenopyrite + brown sphalerite, (2) middle, white (vein) to clear quartz (vug) + base-metal sulfides + electrum + argentite, (3) late, calcite + pyrite + native silver. Mineralogic and fluid inclusion data indicate that gold-silver minerals were deposited at temperatures from 210° to 250° with salinities of 4 to 5 wt. % equiv. NaCl and log fs_2 values from −14.0 to −12.2 atm. The linear relationship between homogenization temperature and salinity data indicates that gold-silver deposition was a result of meteoric water mixing. Ore mineralization occurred at pressure conditions of about 70 bars, which corresponds to the mineralization depths of about 260 m to 700 m. There is a remarkable decrease of the calculated $\delta^{18}O$ values of water from 1.3 to -9.7‰ in hydrothermal fluid with increasing paragenetic time. This indicates a progressive increase of meteoric water influx in the hydrothermal system at the Sanjeon deposit. Oxygen-hydrogen, sulfur, and carbon isotope values of hydrothermal fluids indicate that the ore mineralization was formed largely from meteoric waters with the contribution of sulfur and carbon from a deep igneous source.

INTRODUCTION

The Sanjeon Au-Ag mine is located approximately 20 km northeast of Wonju, Gangwondo. The mining operation was most active during the collonial age, but has been done intermittently until 1990. It is now closed. Ore grades of the mine are estimated to be 1.4 to 7.6 g/t Au and 51 to 156 g/t Ag (KMPC, 1987). Ore reserves are unknown.

In this study, we document the nature and physiochemical conditions of mineralization and determine the origin of ore-forming fluids at the Sanjeon deposit.

GEOLOGY AND ORE DEPOSIT

The geology of the Sanjeon Au-Ag deposit is mainly composed of Cretaceous igneous rocks (biotite granite and quartz porphyry) (Fig. 1). Biotite granite lies in the eastern and northern part of the studied district, and consists of quartz,

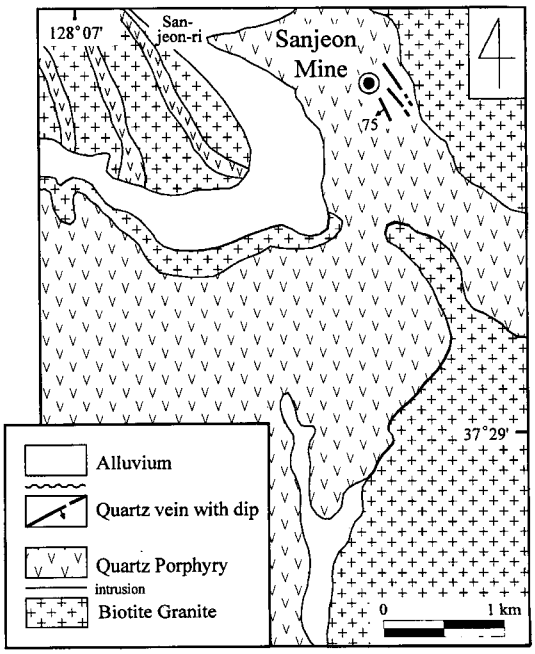

Fig. 1. Simplified geological map of the Sanjeon Au-Ag mine area.

* Department of Mineral and Mining Engineering, Sangji University, Wonju 220-702, Korea, E-mail: shkim@sangji.ac.kr

** Center for Mineral Resources Research, Korea University, Seoul 136-701, Korea

plagioclase, biotite, and amphibole. A Rb-Sr age of biotite in this rock yields 102±9 Ma (Lee, 1987), indicating middle Cretaceous age.

A medium-grained quartz porphyry intrudes the biotite granite, and hosts the Sanjeon Au-Ag deposit. The amount of biotite tends to be increased toward the boundary with biotite granite. Though there is no available age data for the quartz porphyry, the close spatial association of the quartz porphyry with the Sanjeon deposit may indicate that ore mineralization occurred in association with the intrusion of quartz porphyry during the late Cretaceous age.

The Sanjeon Au-Ag deposit consists of three subparallel hydrothermal quartz-calcite veins which filled fault-related fractures (generally N20° to 35° W-trending and 70° to 80° SW-dipping) within quartz porphyry. Each vein is quite similar in mineralogy and texture, and is extended up to 1 km horizontally along the strike direction with a average width of about 20 cm. Along the vein margins, hydrothermal wallrock alteration forms envelops (up to 40 cm thick), locally bleaching the wallrock white or green. The alteration is characterized by silicic, sericitic and chloritic assemblages from inner to outer zone.

The ore mineralogy consists mainly of massive base-metal sulfides (pyrite, arsenopyrite, sphalerite, chalcopyrite and galena), electrum, native silver and sulfosalts (tetrahedrite and polybasite) with quartz and calcite (Fig. 2). Ore veins exhibit relatively complex textures such as crustification, brecciation, and open vugs.

VEIN MINERALOGY

The vein mineralization shows an apparent variation of mineral assemblages with paragenetic time: (1) early, white quartz + pyrite + arsenopyrite + brown sphalerite, (2) middle, white (vein) to clear quartz (vug) + base-metal sulfides + electrum + argentite, (3) late, calcite + pyrite + native silver. The middle mineralization represents the main Au-Ag-depositing period (Fig. 3). Electron microprobe analyses of arsenopyrite, sphalerite and electrum are shown in Tables 1, 2 and 3, respectively.

Early mineralization consists of white vein

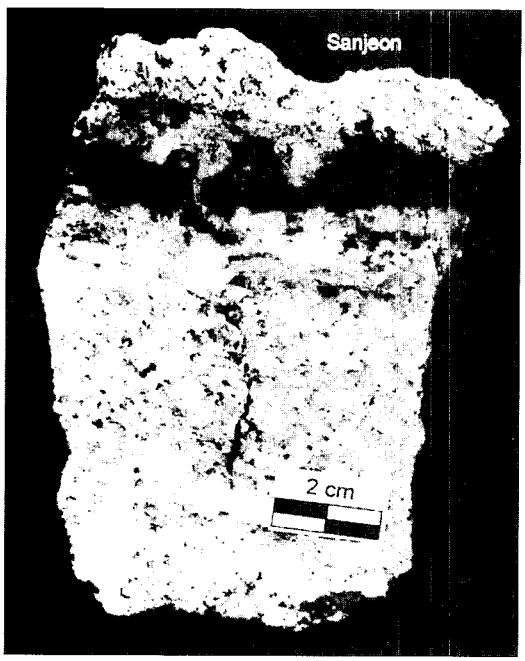

Fig. 2. Photographs of representative ore specimens showing occurrence of white quartz (white) and sulfide minerals (black) in the middle mineralization.

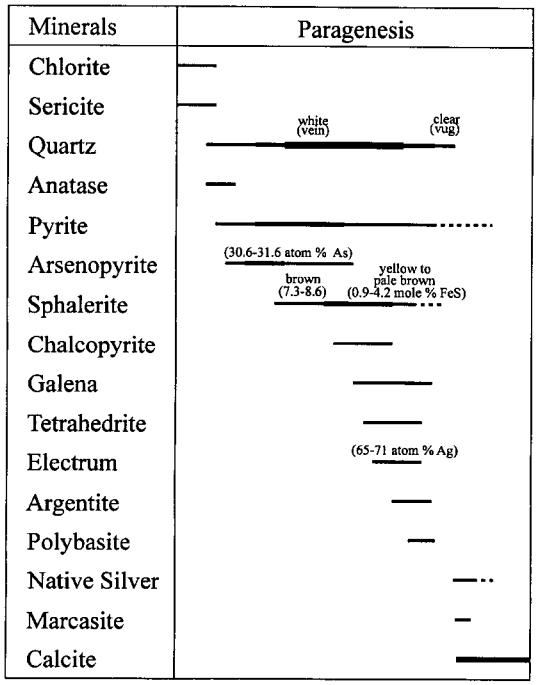

Fig. 3. Generalized paragenetic sequence of hypogene minerals from the Sanjeon mine. Width of lines corresponds to relative abundance.

Table 1. Chemical compositions of arsenopyrite from the Sanjeon Au-Ag mine.

Sample No.	Weight %					Atomic %				Associated mineral
	Fe	As	Sb	S	Total	Fe	As	Sb	S	
SJ 15	34.99	43.43	0.00	21.75	100.17	33.24	30.75	0.00	36.00	py+sp
	35.02	44.10	0.14	21.49	100.75	33.23	31.19	0.06	35.52	
SJ 22	34.81	44.50	0.00	21.16	100.47	33.20	31.64	0.00	35.15	
	35.43	43.15	0.00	21.60	100.18	33.68	30.57	0.00	35.75	

py; pyrite, sp; sphalerite.

Table 2. Chemical compositions of sphalerite from the Sanjeon Au-Ag mine.

Sample No.	Weight %							Mole %					Associated minerals
	Zn	Fe	Mn	Cd	Cu	S	Total	ZnS	FeS	MnS	CdS	CuS	
SJ 6	65.67	0.99	0.00	0.00	0.14	32.91	99.71	98.06	1.73	0.00	0.00	0.21	py+el+arg
	64.95	2.12	0.00	0.00	0.36	33.19	100.63	95.79	3.66	0.00	0.00	0.55	
	64.77	1.23	0.02	0.00	0.33	32.45	98.80	97.29	2.17	0.03	0.00	0.51	
	65.26	0.80	0.00	0.20	0.08	32.81	99.15	98.29	1.40	0.00	0.18	0.13	
SJ 9	61.40	4.81	0.00	0.71	0.00	32.83	99.74	91.05	8.34	0.00	0.61	0.00	py+asp
	62.65	4.28	0.13	0.34	0.13	33.20	100.72	91.94	7.35	0.23	0.29	0.19	
	61.03	4.92	0.04	0.11	0.07	33.08	99.23	91.14	8.60	0.06	0.10	0.10	
SJ 13	61.80	5.01	0.05	0.33	0.18	33.36	100.72	90.75	8.61	0.09	0.28	0.27	py+asp
	62.22	4.21	0.01	0.11	0.01	32.85	99.41	92.54	7.33	0.01	0.10	0.02	
SJ 20	65.22	0.67	0.02	0.53	0.24	32.57	99.24	97.96	1.17	0.04	0.46	0.36	py+el+arg
	66.65	0.95	0.13	0.69	0.14	33.34	101.90	97.36	1.62	0.22	0.59	0.21	
	64.64	1.07	0.00	0.27	0.22	32.80	99.00	97.53	1.89	0.00	0.24	0.34	
	65.61	0.52	0.07	0.62	0.00	32.42	99.24	98.43	0.91	0.12	0.54	0.00	
	65.84	0.81	0.00	0.81	0.01	32.77	100.24	97.87	1.41	0.00	0.70	0.02	
	65.40	0.98	0.07	0.61	0.34	32.95	100.34	97.14	1.70	0.12	0.53	0.52	
SJ 41	65.30	1.69	0.08	0.16	0.01	32.97	100.21	96.77	2.93	0.14	0.14	0.02	py+el+arg
	65.03	1.66	0.03	0.00	0.40	33.12	100.24	95.45	2.89	0.05	0.00	0.61	
	65.68	1.56	0.01	0.11	0.13	33.11	100.61	96.99	2.69	0.02	0.10	0.20	
	67.37	0.73	0.02	0.07	0.00	33.39	101.58	98.66	1.24	0.04	0.06	0.00	
SJ 47	65.77	0.76	0.07	0.68	0.16	31.85	99.29	97.73	1.32	0.12	0.59	0.24	py+el+arg
	60.95	2.41	0.00	0.63	2.38	31.71	98.08	91.53	4.24	0.00	0.55	3.68	
	65.27	0.84	0.04	0.51	0.25	31.80	98.72	97.62	1.48	0.07	0.45	0.39	
	64.65	1.09	0.04	0.69	0.53	31.59	98.57	96.63	1.90	0.06	0.60	0.81	
	65.40	0.33	0.13	0.46	0.20	32.46	99.97	96.78	2.31	0.22	0.39	0.30	

arg; argentite, asp; arsenopyrite, el; electrum, py; pyrite.

Table 3. Chemical compositions of electrum from the Sanjeon Au-Ag mine.

Sample No.	Weight %			Atomic %			Associated mineral
	Ag	Au	Total	Ag	Au	Ag/Au	
SJ 41	54.48	46.05	100.53	68.36	31.64	2.16	py+sp+arg
	52.41	47.47	99.88	66.84	33.16	2.02	
	53.76	46.40	100.16	67.90	32.10	2.12	
	49.54	48.95	98.49	64.89	35.11	1.85	
	56.19	46.82	100.02	67.47	32.53	2.07	
	57.36	43.64	101.00	70.59	29.41	2.40	

arg; argentite, py; pyrite, sp; sphalerite.

quartz, pyrite, arsenopyrite and sphalerite, and contains the altered wallrock fragments. Fine- to coarse-grained pyrite is the most abundant sulfide and occurs as aggregates with arsenopyrite and sphalerite near the vein margin. Euhedral to subhedral arsenopyrite (30.57 to 31.64 atom % As) is closely associated with pyrite and iron-rich, brown sphalerite (7.3 to 8.6 mole % FeS). Rarely, anatase is locally disseminated as dots and/or thin veinlets cutting the altered quartz porphyry.

Middle mineralization is characterized by the occurrence of white quartz showing comb structure and yellow to pale brown sphalerite. It is composed of white (vein) to clear (vug) quartz, base-metal sulfides (pyrite, sphalerite, chalcopyrite and galena), electurm, argentite and sulfosalts (tetrahedrite and polybasite). Yellow to pale brown, iron-poor sphalerite (0.9 to 4.2 mole % FeS) commonly occurs as anhedral aggregates, and are closely associated with pyrite, chalcopyrite, galena and electrum. Electrum (64.9 to 70.6 atom % Ag) occurs as fine irregular grains and fills the fractures within early pyrite. It is commonly associated with pyrite, sphalerite, galena and argentite. Fine-grained chalcopyrite crosscut early pyrite and sphalerite in the form of thin veinlets.

Late vein mineralogy consists of calcite and small amounts of pyrite and native silver. Fine-grained cubic pyrite, native silver, and rhombic calcite occupy the quartz vug during the closure of mineralization, and rarely coat and/or overgrow the vug quartz, although they do not coexist together at a single locality.

FLUID INCLUSION STUDIES

About 280 fluid inclusions in 21 samples of quartz, sphalerite and calcite were examined in order to document the composition and temperature ranges of hydrothermal fluids during the mineralization of the Sanjeon mine. Microthermometric data were obtained using a Linkam THMSG 600 gas-flow heating/freezing system. The size of fluid inclusions is variable and ranges from 5 to 20 micrometer (mean 10 μm). The phenomena of double-freezing and other visual criteria for detecting CO_2 clathrate do not recognized. The inclusions do not contain daughter minerals. Homogenization temperatures and ice melting temperatures have standard errors of ±1.0°C and ±0.2°C, respectively. Salinity data are reported based on freezing point depression in the system H_2O-NaCl (Bodnar, 1993).

Two types of fluid inclusions were recognized based on the relative volume proportions of phases at room temperature: liquid-rich (type I) and vapor-rich (type II) inclusion (Nash, 1972). Type I fluid inclusion is liquid-rich bi-phase inclusions with a vapor bubble of 5 to 20 volume percent (usually 10 vol. %), and homogenizes to the liquid phase. Type II fluid inclusion is vapor-rich bi-phase inclusion with a vapor bubble of 60 to 90 volume percent, and homogenizes to the vapor phase. Type I inclusion occurs as both primary and secondary inclusions, whereas type II inclusion occurs only as primary inclusions. In the early mineralization, the coexistence of type II and type I inclusions suggests that boiling of fluids occurred.

Microthermometric data

Microthermometric data of fluid inclusions are shown in Figs. 4 and 5. Homogenization temperatures of primary type I inclusions in quartz and

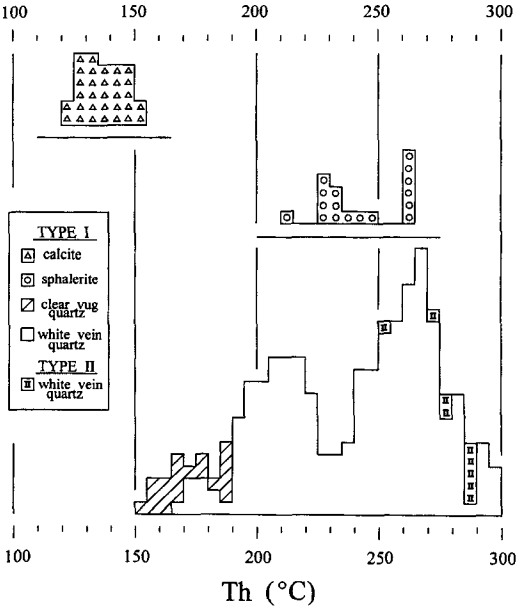

Fig. 4. Frequency diagram of homogenization temperatures of fluid inclusions in vein minerals from the Sanjeon Au-Ag mine.

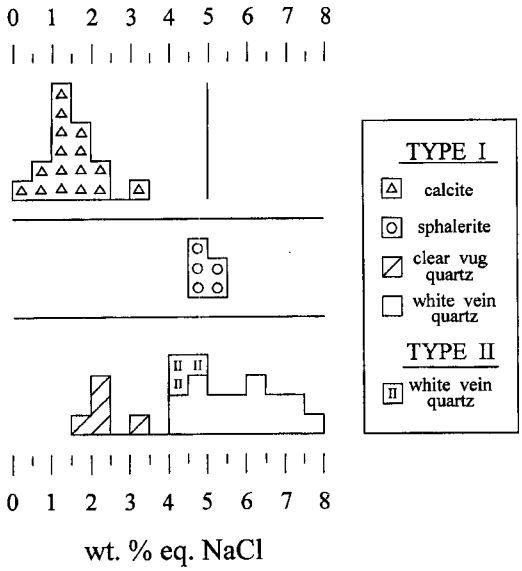

Fig. 5. Frequency diagram of salinities of fluid inclusions in vein minerals from the Sanjeon Au-Ag mine.

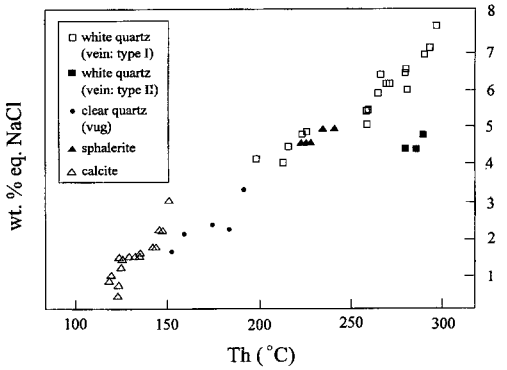

Fig. 6. Diagram showing homogenization temperature versus salinity of fluid inclusions in quartz, sphalerite and calcite from the Sanjeon Au-Ag mine.

sphalerite range from 152° to 297°C (white vein quartz, 168° to 297°C; clear vug quartz, 152° to 188 °C; sphalerite, 211° to 264°C). Primary type II inclu- sions in white vein quartz homogenizes at narrow temperature range from 254° to 286°C. Primary type I inclusions in calcite have homogenization temperatures of 121° to 154°C. Salinities of primary type I inclusions in quartz and sphalerite range from 1.6 to 7.5 wt. % equiv. NaCl (white vein quartz, 4.2 to 7.5; clear vug quartz, 1.6 to 3.4; sphalerite, 4.6 to 5.0). Salinities of primary type II inclusions in white vein quartz range from 4.4 to 4.8 wt. % equiv. NaCl. Salinity of type I fluid inclusions in calcite ranges from 0.4 to 3.0 wt. % equiv. NaCl.

Temperature variations and composition of hydrothermal fluids

Fluid inclusion data indicate that mineralization evolved from high temperature (≈300°C) to lower temperature (≈120°C). Heating data from fluid inclusions reveal that ore-forming fluid has a tendency of decreasing homogenization temperature with time through mineralization. The salinity data also show the similar pattern. During the early mineralization, type II and type I inclusions in white vein quartz occur as close spatial proximity. These inclusions homogenize at similar temperatures (250° to 290°C), which indicate that boiling has occurred in early mineralization. This boiling might have resulted from the pressure decrease in response to fracturing of veins. Homogenization temperatures of yellow to pale brown sphalerite closely associated with electrum, range from 210° to 260°C, which imply that gold was precipitated at these temperature range. The good linear relationship between homogenization temperature and salinity indicate the cooling and dilution of ore fluid by mixing with an external meteoric water (Fig. 6). We consider that gold and base-metal deposition at Sanjeon was a combined result of boiling and meteoric water mixing.

Pressure-depth conditions

Evidence of a temporal fluid boiling at temperatures of 280±10°C during the deposition of early white quartz allows us to determine a pressure-depth estimate at the time of mineralization. The data of Hass (1971) for the system H_2O-NaCl, combined with temperature and salinity data (4.4 to 4.8 wt. % equiv. NaCl), indicate a fluid pressure of about 70 bars. This pressure corresponds to mineralization depths of about 260 m and 700 m under lithostatic and hydrostatic pressure regimes, respectively. The common presence of open vugs, however, suggests that pressure during the late mineralization was essentially hydrostatic because the ore fluids could circulate freely to the surface.

GEOCHEMICAL CONDITIONS OF MINERALIZATION

Temperature and sulfur fugacity

Ranges of temperature and sulfur fugacity (fs_2) were estimated from phase relations and mineral compositions in the system Fe-As-S (Kretschmar and Scott, 1976), Fe-Zn-S (Barton and Toulmin, 1966), Fe-S (Helgeson, 1969) and Au-Ag-S (Barton and Toulmin, 1964), as shown in Fig. 7.

In the early mineralization, arsenopyrite (30.6 to 31.6 atom % As), pyrite and iron-rich sphalerite (7.3 to 8.6 mole % FeS) coexist. This pregold assemblage indicates the temperatures of 360° to 410°C and log fs_2 values of −7.8 to −6.0 atm.

Electrum (N_{Ag} = 0.65 to 0.71) + yellow to pale brown, iron-poor sphalerite (0.9 to 5.0 mole % FeS) + pyrite + argentite assemblage in the middle mineralization was precipitated within a temperature range of 170° to 250°C and log fs_2 values of −15.8 to −12.2 atm. This temperature range of gold mineralization is in good agreement with that estimated from homogenization temperatures of fluid inclusions (Fig. 4). In summary, there is a systematic decrease in log fs_2 values (from −6.0 to −15.8 atm) and temperature (from 410° to 170 °C) with increasing time during the hydrothermal mineralization.

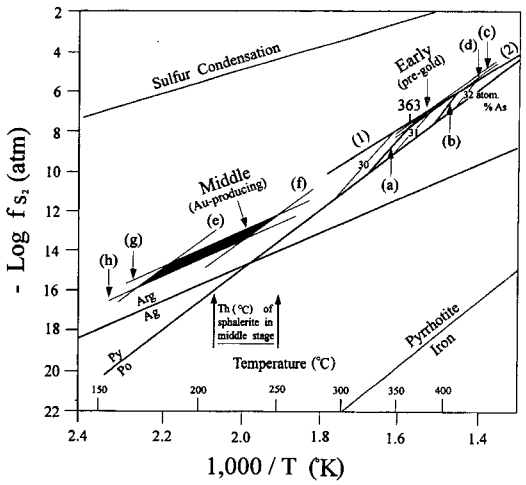

Fig. 7. Sulfur fugacity versus temperature diagram showing sulfidation reactions pertinent to mineral assemblages of the Sanjeon mine. Curves (1) and (2) represent the pyrite + arsenic = arsenopyrite and pyrite + liquid = arsenopyrite equilibria, respectively (Kretschmar and Scott, 1976). Compositional isopleths for arsenopyrite (atom % As) are (a); 30.6 percent, (b); 31.6 percent. Isopleths for sphalerite (mole % FeS) are (c); 7.3 percent, (d); 8.6 percent, (e); 0.9 percent, (f); 4.2 percent. Isopleths for electrum (atom % Ag) are (g); 0.65, (h); 0.71. Ag; native silver, Arg; argentite, Po; pyrrhotite, Py; pyrite, Th (°C); homogenization temperature of fluid inclusions.

Oxygen fugacity and total sulfur concentration

It is possible to define limits of oxygen fugacity and H_2S concentration of gold-depositing fluids using the fs_2-fo_2 diagram at 250°C (Fig. 8). Combined with log fs_2 values defined by sphalerite composition (Fig. 7), the occurrence of pyrite but the absence of graphite, pyrrhotite and magnetite in gold-depositing period allow the permissible range of log fo_2 values between −39 to −36 atm. Using the reaction $H_2S(aq) + 1/2\ O_2 = H_2O + 1/2\ S_2$, log molality of H_2S is calculated to be about −3.5 to −2.0. Equilibrium constants used for constraining reactions are from Robie and Waldbaum (1968) and Helgeson (1969). Therefore, the log molality of H_2S near −3 may be taken as an

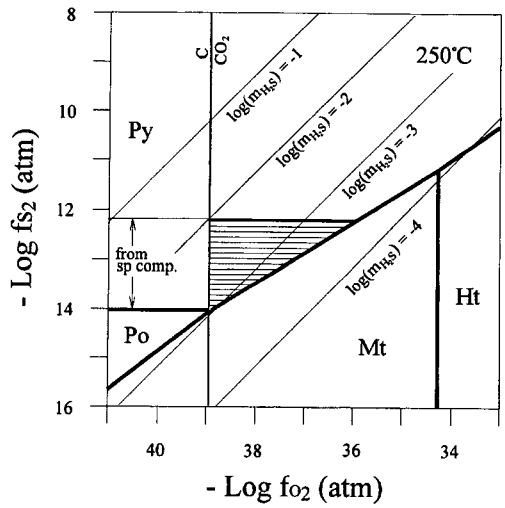

Fig. 8. Diagram showing sulfur fugacity versus oxygen fugacity at 250°C relevant to gold-depositing fluids of the Sanjeon mine (shaded region). Thick solid lines indicate the stability field of minerals in the system Fe-O-S; thin solid lines and the total concentration of $H_2S(aq)$. Ht; hematite, Mt; magnetite, Po; pyrrhotite, Py; pyrite, sp comp.; sphalerite composition.

approximation of the concentration of total sulfur in the ore fluid.

pH

The pH of fluids that are responsible for gold mineralization was probably controlled by the assemblage quartz + K-feldspar + muscovite. The likely value for the molality of potassium ion in the fluid (mK^+) is estimated to be about 0.05 m at 250°C by combining the salinity data (Fig. 5) with chemical characteristics of natural hydrothermal systems (Ellis and Mahon, 1967; Fournier and Truesdell, 1973). The pH of this fluid is calculated to be about 5 to 6 at 250°C (Helgeson, 1969) (Fig. 9). The most important means of transporting the gold are as either chloride or sulfide complexes. Sulfide complexes of gold are favored in shallow, low-temperature (< 300°C), low salinity, reducing ore fluids (Seward, 1973, 1984). Using the experimental data from Seward (1973, 1984), the calculated solubilities of gold bisulfide, $Au(HS)_2^-$, is approximately 0.01 to 0.1 ppm.

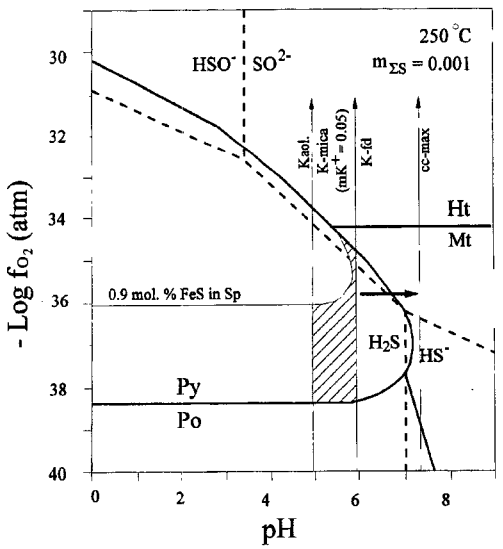

Fig. 9. Isothermal (250°C) pH versus oxygen fugacity diagram showing stability relations of oxide and sulfide minerals and sulfur species in solution at $m\Sigma S$; 0.001. Vertical solid lines indicate the sericite-K feldspar-kaolinite reaction (mK^+; 0.05) and calculated maximum solubility of calcite (cc-max). Shaded area represent the probable fluid chemistries. Sp; sphalerite, K-fd; K feldspar, K-mica; sericite, Kaol.; kaolinite.

If hydrothermal fluids completely equilibrated with the calcite in wall rocks, pH would be controlled by the maximum solubility of calcite. Utilizing equilibrium constants and activity coefficients (Helgeson, 1969; Ohmoto, 1972), calculations indicate that a fluid in equilibrium with calcite at 250°C would have a pH of 7.3 (Fig. 9). Computations, therefore, indicate that pH of ore-forming fluids possibly have increased from about 5.5 to 7.3 during the mineralization. Such an increase in pH could be an effective mechanism of precipitation of sulfide minerals.

STABLE ISOTOPE STUDIES

In order to elucidate the origin and evolution of hydrothermal fluids in the Sanjeon Au-Ag deposit, we measured the sulfur isotope compositions of 2 sulfides, carbon isotope composition of 1 calcite, the oxygen isotope compositions of 4 quartz and 1 calcite, and the hydrogen isotope compositions of 2 fluid inclusion waters extracted from quartz. Standard techniques for extraction and analysis were used as described by McCrea (1950), Grinenko (1962), Taylor and Epstein (1962) and Hall and Friedman (1963). Isotope data are reported in standard δ notation relative to the Canyon Diablo troilite (CDT) standard for sulfur, the Pee Dee belemnite (PDB) standard for carbon, and the Vienna SMOW standard for oxygen and hydrogen. The standard error of each analysis is approximately ±0.1 per mil for sulfur, carbon and oxygen, and ±0.2 per

Table 4. Sulfur isotope data of sulfide minerals from the Sanjeon Au-Ag mine.

Sample No.	Mineral	$\delta^{34}S$(‰)	T(°C)[1]	$\delta^{34}S_{H2S}$(‰)[2]	Remark
SJ 18	pyrite	0.4	300	−0.8	early
	pyrite	−1.2	300	−2.4	early

[1] Based on fluid inclusion temperatures
[2] Based on sulfur isotope fractionation equations compiled by Ohmoto and Rye (1979)

mil for hydrogen.

Sulfur isotope

Sulfur isotope data of hand-picked sulfides (2 pyrite) are shown in Table 4. The sulfides have nearly uniform $\delta^{34}S$ (−1.2 to 0.4 permil). Based on the fluid inclusion homogenization temperatures, $\delta^{34}S$ values of H_2S in ore fluids are calculated (using the compiled data of Ohmoto and Rye, 1979) to fall in the range of −2.4 to −0.8 per mil.

Carbon, oxygen and hydrogen isotopes

The $\delta^{13}C$, $\delta^{18}O$ and δD values for examined minerals and their inclusion fluids are summarized in Table 5. Calcite has a $\delta^{13}C$ value of −4.8 ‰. Coupled with fluid inclusion homogenization temperatures, the calcite-CO_2 carbon isotope fractionation of calcite (Friedman and O'Neil, 1977) yields the $\delta^{13}C_{CO2}$ value of −5.8‰, possibly indicating a deep igneous source of carbon (Pineau *et al.*, 1976; Field and Fifarek, 1986).

Measured $\delta^{18}O$ value of calcite is 2.5‰. Using the calcite-water (Friedman and O'Neil, 1977) oxygen isotope fractionation equation, coupled with temperature estimate based on fluid inclusions, the calculated $\delta^{18}O$ value of water in equilibrium with calcite is −9.7‰. The $\delta^{18}O$ values of quartz are 3.6 to 8.9‰. Using the quartz-water oxygen isotope fractionation equation of Matsuhisa *et al.* (1979), the oxygen isotope compositions of waters in hydrothermal fluids is calculated to fall in the range −5.1 to 1.3‰. Fluid inclusion waters were extracted by crushing from quartz samples and analyzed for hydrogen isotope composition. The D values of inclusion waters are −77 to −73‰.

Interpretation of oxygen and hydrogen isotope results

The calculated $\delta^{18}O_{water}$ values show a systematic decrease with increasing paragenetic time and decreasing temperature, from 1.3 to −9.7‰. This trend indicates an overall progressive increase of meteoric water influx in the hydrothermal system (Table 5; Fig. 10).

The measured and calculated $\delta^{18}O_{water}$ and δD_{water} data from quartz fall toward the meteoric

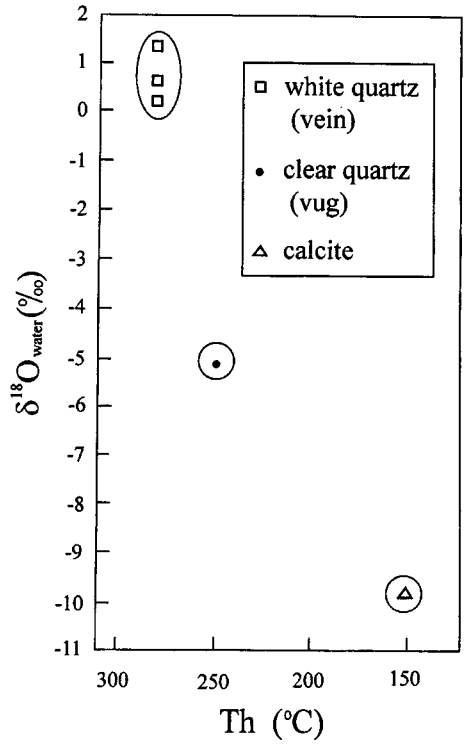

Fig. 10. Temperature versus oxygen isotope diagram displaying the systematic decrease of $\delta^{18}O$ values of water in the Sanjeon hydrothermal fluids with increasing paragenetic time.

Table 5. Carbon, oxygen and hydrogen isotope data of calcite and quartz from the Sanjeon Au-Ag mine.

Sample No.	Mineral	$\delta^{13}C$(‰)	$\delta^{18}O$(‰)	T(°C)[1]	$\delta^{18}O_{water}$(‰)	δD_{water}(‰)[2]	Remark
SJ 7	quartz	–	8.9	280	1.3	−77	early
	quartz	–	3.6	250	−5.1	−73	middle
SJ 17	quartz	–	7.8	280	0.2	–	early
	quartz	–	8.2	280	0.6	–	early
SJ 23	calcite	−4.8	2.5	150	−9.7	–	late

[1] Based on fluid inclusion temperatures

[2] Based on oxygen isotope fractionation factors: quartz-water, Matsuhisa *et al.* (1979); calcite-water, Friedman, O'Neil (1977)

water line on a conventional H versus O isotope diagram, indicating the mixing of highly exchanged meteoric water with less exchanged meteoric water. We conclude that the hydrothermal fluids of the Sanjeon Au-Ag deposit derived mainly from meteoric water. As indicated by sulfur and carbon isotope data, however, magmatic fluids at deposits provided the gases such as sulfur and carbon during the circulation of meteoric water.

CONCLUSION

1. The Au-Ag deposit of the Sanjeon mine is composed of three subparallel hydrothermal quartz-calcite veins which were formed by the filling of fault-related fractures (generally N20° to 35°W-trending and 70° to 80° SW-dipping) within quartz porphyry.

2. The cooling and dilution of ore fluid during the middle mineralization resulted from progressive mixing with an external meteoric water, as indicated by the positive relationships between homogenization temperatures and salinities.

3. Mineral assemblages and fluid inclusions data indicate that gold deposition during the middle mineralization occurred at temperature from 210° to 250°C with salinities of 4 to 5 wt. % equiv. NaCl. The ore-forming fluids of middle mineralization had log fs_2 values of −14.0 to −12.2 atm.

4. The calculated $\delta^{18}O_{water}$ values of hydrothermal fluids show a systematic decrease with time, 1.3 to −9.7‰. This trend indicates a progressively increasing amounts of meteoric water interaction in the hydrothermal system. The $\delta^{18}O_{water}$ and δD_{water} data also fall toward the meteoric water line, indicating the mixing of highly exchanged meteoric water with less exchanged meteoric water or unexchanged meteoric water. However, carbon and sulfur isotope data shows the involvement (mixing) of magmatic components during the meteoric water circulation.

ACKNOWLEDGEMENT

This research was supported by the Center for Mineral Resource Research (CMR). We also thank the Sangji University for partial support.

REFERENCES

Barton, P.B., Jr. and Toulmin, P., III (1964) The electrum tarnish method for determination of the fugacity of sulfur in laboratory sulfide systems. Geochim. Cosmochim. Acta, v. 28, p. 619-640.

Barton, P.B., Jr. and Toulmin, P., III (1966) Phase relations involving sphalerite in the Fe-Zn-S system. Econ. Geol., v. 61, p. 815-849.

Bodnar, R.J. (1993) Revised equation and table for determining the freezing point depression or H_2O-NaCl solutions. Geochim. Cosmochim. Acta, v. 57, p. 683-684.

Drummond, S.E., and Ohmoto, H. (1985) Chemical evolution and mineral deposition in boiling hydrothermal systems. Econ. Geol., v. 80, p. 126-147.

Ellis, A.J., and Mahon, W.A.J. (1967) Natural hydrothermal systems and experimental hot water/rock interaction (III). Geochim. Cosmochim. Acta, v. 31, p. 519-538.

Field, C.W. and Fifarek, R.H. (1986) Light stable-isotope systematics in the epithermal environment. Rev. Econ. Geol., v. 2, p. 99-128.

Fournier, R.O., and Truesdell, A.H. (1973) An empirical Na-K-Ca geothermometer for natural waters. Geochim. Cosmochim. Acta, v. 37, p. 1255-1275.

Friedman, I. and O'Neil, J.R. (1977) Compilation of stable isotope fractionation factors of geochemical interest. In Fleisher, M., ed., Data of geochemistry, Sixth Edition, U.S.G.S. Prof. Paper 440-KK, p. KK4-KK12.

Grinenko, V. A. (1962) Preparation of sulfur dioxide for isotopic analysis. Zeitschr. Neorgan. Khimii, v. 7, p. 2478-2483.

Hall, W.E., and Friedman, I. (1963) Composition of fluid inclusions, Cave-in rock fluorite district, Illinois and upper Mississippi valley zinc-lead district. Econ. Geol., v. 58, p. 886-911.

Hass, J.L., Jr. (1971) The effect of salinity on the maximum thermal gradient of a hydrothermal system at hydrostatic pressure. Econ. Geol., v. 66, p. 949-946.

Helgeson, H.C. (1969) Thermodynamics of hydrothermal systems at elevated temperatures and pressures. Am. Jour. Sci., v. 267, p. 729-804.

Korea Mining Promotion Corporation (1987) Gold and silver deposits in Korea, v. 10, p. 173-174.

Kretschmar, U., and Scott, S.D. (1976) Phase relations involving arsenopyrite in the system Fe-As-S and their application. Am. Min., v. 14, p. 364-386.

Lee, D.S. (1987) Geology of Korea. Kyohaksa Pub., Seoul, Korea, 514 p.

Matsuhisa, T., Goldsmith, J.R., and Clayton, R.N. (1979) Oxygen isotopic fractionation in the system quartz-albite-anorthite-water. Geochim. Cosmochim. Acta, v. 43, p. 1131-1140.

McCrea, J.M. (1950) The isotope chemistry of carbonates and a paleotemperature scale. Jour. Chem. Physics, v. 18, p. 849-857.

Nash, J.T. (1972) Fluid inclusion studies of some gold deposits in Nevada. U.S.G.S. Prof. Paper 800-C, p. 15-19.

Ohmoto, H. (1972) Systematics of sulfur and carbon isotopes in hydrothermal ore deposits. Econ. Geol., v. 67, p. 551-578.

Ohmoto, H. and R.O. Rye (1979) Isotopes of sulfur and carbon, Geochemistry of Hydrothermal Ore Deposits. In Barnes, H.L., 2nd ed., John Wiley & Sons, Inc. p. 509-567.

Pineau, F., Javoy, M. and Bottinga, Y. (1976) $^{13}C/^{12}C$ ratios of rocks and inclusions in popping rocks of the Mid-Atlantic ridge and their bearing on the problem of isotopic composition of deep-seated carbon. Earth Planet Sci. Letters, v. 29, p. 413-421.

Robie, R.A. and Waldbaulm, D.R. (1968) Thermodynamic properties of minerals and related substances at 298.15°K(25°C) and one atmosphere (1.013 bars) pressure and at higher temperature. U.S.G.S. Bull., 1259, 256p.

Seward, T.M. (1973) Thio complexes of gold in hydrothermal ore solutions. Geochim. Cosmochim. Acta, v. 37, p. 379-399.

Seward, T.M. (1984) The transport and deposition of gold in hydrothermal systems. In Foster, R. P., de., Gold '82: Rotterdam, A.A. Balkema Pub., p. 165-181.

Taylor, H.P., Jr. And Epstein, S. (1962) Relationship between $^{18}O/^{16}O$ ratios in coexisting minerals in igneous and metamorphic rocks. Part I. Principles and experimental results. Geol. Soc. Am. Bull., v. 73, p. 461-480.

1998년 12월 24일 원고접수, 1999년 7월 10일 게재승인.

산전 금-은 광상에 관한 광물 및 지화학적 연구

김세현* · 최영천* · 염승준**

요 약 : 산전 금-은 광상은 석영 반암내에 발달된 열극을 충진한 석영+방해석의 열수맥상광상이다. 광화작용은 단일 시기에 형성되었으며, 시간에 따라 다음과 같이, (1) 초기, 백색 석영+황철석+유비철석 + 섬아연석; (2) 중기, 백색-투명 석영+ 황화광물 (황철석, 섬아연석, 황동석, 방연석)+에렉트럼+휘은석; (3) 후기, 방해석+황철석+자연은의 정출이 있었다. 금-은의 주요 광화기인 중기 광화유체의 온도와 NaCl 상당 염농도는 210°~250°C와 4~5 wt. % 이고, 황분압은 −14.0~−12.2 atm 으로 금-은의 침전은 천수의 혼입작용에 기인한 것으로 보인다. 산소 및 수소동위원소 분석에 의하면, 광화작용이 진행됨에 따라 양자 모두 감소하는 경향을 갖는다. 이는 광화작용이 진행됨에 따라 천수의 혼입이 증가하기 때문으로 해석된다.